Frontiers in Bioscience Landmark

Front. Biosci. (Landmark Ed) **2026**; 31(5): 49465
https://doi.org/10.31083/FBL49465

Original Research

Conditional Immortalization of Human Cardiac Fibroblasts for Pro-Fibrotic and Anti-Fibrotic Drug Screening

Sushan Wang[1,2,†], Ruijuan Han[3,†], Rui Guo[2], Cheng Wang[3], Wenan Kang[2], Jia Liu[1,2,*,§], Canling Long[2,*,§]

[1]School of Life Sciences, Anhui Medical University, 230601 Hefei, Anhui, China
[2]Central Laboratory, School of Medicine, The Second Affiliated Hospital, The Chinese University of Hong Kong, Shenzhen & Longgang District People's Hospital of Shenzhen, 518172 Shenzhen, Guangdong, China
[3]Department of Cardiology, School of Medicine, The Second Affiliated Hospital, The Chinese University of Hong Kong, Shenzhen & Longgang District People's Hospital of Shenzhen, 518172 Shenzhen, Guangdong, China
*Correspondence: liujia870702@126.com (Jia Liu); lcl3210@126.com (Canling Long)
[†]These authors contributed equally.
[§]These authors contributed equally.
Academic Editor: Esteban C. Gabazza
Submitted: 26 December 2025 Revised: 17 March 2026 Accepted: 23 March 2026 Published: 30 April 2026

Abstract

Background: The development of anti-fibrotic therapies for heart failure is hindered by the absence of phenotypically stable and scalable human cardiac fibroblast (CFB) models suitable for pre-clinical drug screening. This study aimed to establish and validate a conditionally immortalized CFB (iCFB) cell line for screening cardiac fibrosis drugs. **Methods**: An iCFB line was generated using a doxycycline (dox)-inducible system. The cellular characteristics were evaluated using molecular, protein, and functional analyses. The utility of the model was assessed by exposure to multiple pro-fibrotic stimuli (transforming growth factor-β1 (TGF-β1), angiotensin II, and palmitic acid) and two anti-fibrotic compounds (N-[(1R)-1,2,3,4-tetrahydro-1-naphthalenyl]-1H-benzimidazol-2-amine [NS8593] and pirfenidone). **Results**: iCFB proliferation was tightly regulated by dox. Upon dox withdrawal, the iCFBs reverted to a quiescent state and exhibited a molecular expression profile (collagen type I alpha 1 chain [*COL1A1*], periostin [*POSTN*], gap junction protein alpha 1 [*GJA1*], and T-box transcription factor 20 [*TBX20*]) comparable to that of primary CFBs. This phenotypic fidelity, along with a robust capacity for TGF-β1-induced myofibroblast differentiation, was maintained during long-term culture up to population doubling 60. The model responded consistently to diverse pro-fibrotic stimuli, confirming the anti-fibrotic efficacy of the transient receptor potential melastatin 7 (TRPM7) inhibitor, NS8593, and demonstrating the therapeutic potential of the repurposed drug pirfenidone. **Conclusions**: We developed a novel iCFB model that integrates long-term expandability, high biological fidelity, and broad responsiveness to fibrotic signaling. This robust platform is well-suited for mechanistic studies and drug screening, thereby facilitating and accelerating the discovery of anti-fibrotic therapeutics.

Keywords: cell immortalization; fibroblasts; fibrosis; myofibroblasts; cell transdifferentiation; drug evaluation

1. Introduction

Cardiac fibroblasts (CFBs) are the principal extracellular matrix (ECM) producers in the heart and exhibit considerable plasticity. Under physiological conditions, they play a critical role in maintaining normal cardiac structure and function [1–3]. However, in response to pathological stimuli such as myocardial injury or pressure overload, they become activated and differentiate into cardiac myofibroblasts (CMFBs) [4–6]. Activated CMFBs exhibit sustained proliferative activity and secrete excess collagen and other ECM components [7–10]. Although this response is initially adaptive-for example, by preventing cardiac rupture following myocardial infarction-excess or persistent fibrotic activation increases myocardial stiffness, reduces ventricular compliance, impairs cardiac function, and ultimately contributes to heart failure progression [11–15].

At present, cardiac fibrosis has no specific and effective therapies, underscoring an urgent need for anti-fibrotic drug development [16–19]. Progress in this field is constrained by the limitations of available experimental models. Current assessments of fibrosis primarily rely on animal models and *in vitro* assays employing fibroblasts [20]. However, animal-derived cellular models exhibit substantial species-specific differences compared to human cells, and primary human CFBs (pCFBs) are difficult to obtain in sufficient quantities owing to limited tissue availability, restricted proliferative capacity, and ethical considerations. This creates a critical knowledge gap: the lack of a scalable, phenotypically stable, and physiologically relevant human CFB *in vitro* model that can bridge the translational gap between pre-clinical research and clinical anti-fibrotic drug development and is suitable for high-throughput pro-fibrotic and anti-fibrotic drug screening. As an innovative optimization strategy, conditional immortalization technol-

ogy directly addresses this long-standing technical bottleneck via a drug-controlled reversible gene expression system [21,22]. This strategy enables flexible switching between an immortalized proliferative state for large-scale cell production and a quiescent, primary-cell-like state for functional experiments, thus achieving the unification of long-term scalability and high biological fidelity, which is difficult to realize with existing models. Consequently, the development of a stable, reproducible, and physiologically relevant human-based *in vitro* CFB model using this conditional immortalization approach is essential to accelerate the discovery and evaluation of anti-fibrotic therapeutics.

In this study, we aimed to establish a conditionally immortalized human CFB cell line (iCFB) based on a doxycycline (dox)-inducible system that supports long-term expansion while retaining the key biological characteristics of pCFB. CMFB activation was induced *in vitro* using pro-fibrotic mediators, including transforming growth factor-β1 (TGF-β1), angiotensin II (Ang II), and palmitic acid (PA), to recapitulate core features of the cardiac fibrotic response. The resulting cellular model was subsequently employed for the systematic screening and evaluation of existing drugs and novel compounds for anti-fibrotic efficacy. This approach provides a robust and scalable platform for *in vitro* investigation of cardiac fibrosis and supports future translational research in anti-fibrotic therapy development.

2. Materials and Methods

2.1 Plasmid Construction and Lentiviral Production

The dox-inducible plasmid, pLVET-tTR-KRAB, was obtained from Addgene (Cambridge, MA, USA; plasmid #11644). Based on the gene sequences retrieved from GenBank, the SV40 large T antigen (LT) fragment was synthesized and used to construct a lentiviral shuttle recombinant plasmid. Specifically, the human EEF1A1 promoter and enhanced green fluorescent protein (EGFP)-coding sequence in pLVET-tTR-KRAB were replaced with the collagen type I alpha 2 chain (*COL1A2*) promoter and LT gene, respectively. All plasmid construction and lentiviral packaging procedures were performed using VectorBuilder (Guangzhou, Guangdong, China).

2.2 pCFB Isolation and Primary Culture

pCFBs were isolated from ventricular tissue of a fetus at 14 weeks of gestation. The tissue was donated by the fetal parents with written informed consent. This study was approved by the Ethics Committee of Longgang District People's Hospital of Shenzhen (approval number: 2025101). Cells were cultured in high-glucose Dulbecco's modified Eagle medium (H-DMEM; Gibco, Thermo Fisher Scientific, Waltham, MA, USA; Catalog No. 11965118) supplemented with 10% fetal bovine serum (FBS; Gibco, Catalog No. A5256901), 1% penicillin-streptomycin (Gibco, Catalog No. 15140122), and 10 ng/mL recombinant human basic fibroblast growth factor (bFGF; R&D Systems, Minneapolis, MN, USA; Catalog No. 233-FB) and maintained at 37 °C in a humidified incubator with 5% CO_2. The culture medium was replaced every three days. Upon reaching confluence, pCFBs were passaged at a 1:4 ratio and cells at population doubling 4 (PD4) were used for subsequent experiments.

2.3 pCFB Transduction and iCFB Establishment

The pCFBs at approximately PD4 were transduced with lentiviral vectors carrying the dox-inducible LT expression system. After 24 h of initial culture in the primary cell medium, the medium was replaced with proliferation medium supplemented with 100 ng/mL dox (Sigma-Aldrich, St. Louis, MO, USA; Catalog No. D9891) to induce LT expression. Successfully transduced cells were designated conditional iCFBs and maintained in freshly prepared dox-containing proliferation medium, which was replaced every alternate day. When the cultures reached approximately 90% confluence, they were passaged in a 1:8 ratio.

2.4 pCFB Proliferation Assay

For growth curve analysis, iCFBs and pCFBs were passaged at ratios of 1:8 and 1:4, respectively, upon reaching confluency. To evaluate the proliferation rates and their dependence on LT expression, the cells were seeded at a low density and cultured in medium supplemented with 100 ng/mL dox (iCFBs) or standard culture medium (pCFBs). The cell numbers were quantified at the indicated time points using a cytometer (BodBoge, Guangzhou, Guangdong, China).

2.5 Foreskin Fibroblast Culture

Primary human foreskin fibroblasts (FFBs) were purchased from Jennio Biotech Co., Ltd. (Guangzhou, Guangdong, China; Catalog no. JNO-H0612) and cultured in H-DMEM supplemented with 10% FBS in a humidified incubator at 37 °C with 5% CO_2. The culture medium was replaced every three days. The cells were routinely passaged at a 1:4 ratio when the cultures reached approximately 80% confluence.

All primary cells were routinely tested for mycoplasma contamination using the BeyoDirect™ Mycoplasma qPCR Detection Kit (Beyotime, Shanghai, China; Catalog No. C0303S) and consistently tested negative, as defined by the kit's criteria (sample Ct $>$35). Their identity was confirmed by marker gene expression and/or biological function analyses.

2.6 Immunofluorescence

The cells were fixed with 4% paraformaldehyde in phosphate-buffered saline (PBS), permeabilized with 0.5% Tween-20 in PBS, and blocked with PBS containing 1% bovine serum albumin (Sigma-Aldrich, Catalog No. A8022), and 0.05% Tween-20 (Sangon Biotech, Shanghai,

China; CAS No. 9005-64-5). pCFB, iCFB, and FFB monolayers were incubated overnight at 4 °C with the following primary antibodies: mouse anti-SV40 LT (1:50; Santa Cruz Biotechnology, Dallas, TX, USA; Catalog No. sc-147), anti-Collagen type I (anti-COL-1) (1:200; Proteintech, Wuhan, Hubei, China; Catalog No. 66761-1-Ig), anti-α-smooth muscle actin (anti-α-SMA) (1:200; Proteintech, Catalog No. 67735-1-Ig), and anti-connexin 43 (anti-CX43) (1:50; Proteintech, Catalog No. 80543-1-RR).

After three washes with PBS containing 0.05% Tween-20, the bound primary antibodies were detected using Alexa Fluor 594-conjugated goat anti-mouse IgG (H+L) (1:200; Thermo Fisher Scientific, Catalog No. A-11005). Nuclei were counterstained with Hoechst 33342 (10 µg/mL; Thermo Fisher Scientific, Catalog No. H3570). Fluorescence images were acquired using a Leica STELLARIS 5 confocal laser-scanning microscope (Leica Microsystems).

2.7 Western Blot Analysis

Protein extracts were separated by sodium dodecyl sulfate-polyacrylamide gel electrophoresis (SDS-PAGE) and transferred on 0.22 or 0.45 µm polyvinylidene difluoride (PVDF) membranes (Millipore, Billerica, MA, USA; Catalog No. IPVH00010). After blocking with 5% skim milk in Tris-buffered saline containing Tween-20 (TBST), the membranes were incubated overnight at 4 °C with the following primary antibodies: anti-SV40 LT (1:1000; Santa Cruz Biotechnology, Catalog No. sc-147) and anti-glyceraldehyde-3-phosphate dehydrogenase (anti-GAPDH) (1:5000; Proteintech, Catalog No. 60004-1-Ig).

The membranes were subsequently incubated with horseradish peroxidase (HRP)-conjugated secondary antibody (1:5000; Proteintech, Catalog No. SA00001-0) for 1 h at room temperature. Protein bands were visualized using the Thermo iBright CL1000 imaging system (Thermo Fisher Scientific) with Pierce™ ECL Western Blotting Substrate (Thermo Fisher Scientific, Catalog No. 32209). Band intensities from at least three independent experiments were quantified using the ImageJ software (version 1.46r, National Institutes of Health, Bethesda, MD, USA).

2.8 RNA Isolation and Reverse Transcription-Quantitative Polymerase Chain Reaction (RT-qPCR)

Total RNA was extracted from the cultured cells using AG RNAex Pro Reagent (Accurate Biotechnology, Ningbo, Zhejiang, China) according to the manufacturer's instructions. The isolated RNA was reverse transcribed into complementary DNA (cDNA) using Evo M-MLV RT Premix for qPCR (Accurate Biotechnology). Gene expression levels were determined by RT-qPCR using the SYBR® Green Premix Pro Taq HS qPCR Kit (Accurate Biotechnology). PCR amplification and fluorescence detection were performed using the QuantStudio 3 Real-Time PCR System (Thermo Fisher Scientific). Relative gene expression was calculated using the $2^{-\Delta\Delta Ct}$ method. The primer sequences are listed below. 5′-CAGCCACTAGCCATTGTGGA-3′ (F, gap junction protein alpha 1 [*GJA1*]); 5′-GGCTGTTGAGTACCACCTCC-3′ (R, *GJA1*); 5′-TGACGAGACCAAGAACTGCC-3′ (F, collagen type I alpha 1 chain [*COL1A1*]); 5′-GCACCATCATTTCCACGAGC-3′ (R, *COL1A1*); 5′-GGAGGCAAACAGCTCAGAGT-3′ (F, periostin [*POSTN*]); 5′-GGTGTGTCTCCCTGAAGCAG-3′ (R, *POSTN*); 5′-GTTCCGCTCCTCTCTCCAAC-3′ (F, actin alpha 2 [*ACTA2*]); 5′-TAGTCCCGGGGATAGGCAAA-3′ (R, *ACTA2*); 5′-ACCATCCGGGTGTCCTTTTC-3′ (F, T-box transcription factor 20 [*TBX20*]); 5′-TGACCCTCGATTTGGGGTTG-3′ (R, *TBX20*); 5′-TTGCATCAGCCTGTGGATGT-3′ (F, discoidin domain receptor tyrosine kinase 2 [*DDR2*]); 5′-GAGTCCAGCCAAAGGTCTCC-3′ (R, *DDR2*); 5′-CTCTGGCACGTCTTGACCTT-3′ (F, vimentin [*VIM*]); 5′-TTGCGCTCCTGAAAAACTGC-3′ (R, *VIM*); 5′-AATGGGCAGCCGTTAGGAAA-3′ (F, *GAPDH*); 5′-GCGCCCAATACGACCAAATC-3′ (R, *GAPDH*).

2.9 Collagen-Based Cell Contraction Assay

The collagen-based cell contraction assay was performed using a commercial kit (Cell Biolabs, San Diego, CA, USA; Catalog No. CBA-201) according to the manufacturer's instructions. iCFBs and pCFBs (2.0×10^5 cells per well) were seeded and cultured in the presence or absence of TGF-β1. After 48 h, the collagen gels were photographed and gel surface area was quantified using ImageJ software (version 1.46r, National Institutes of Health).

2.10 Drug Treatment

The iCFBs were cultured in doxycycline-free DMEM for 4 days to suppress LT expression. Thereafter, pCFBs and iCFBs were treated with 10 ng/mL TGF-β1 (R&D Systems, Minneapolis, MN, USA; Catalog No. 240-B), 1 µM Ang II (MedChemExpress, Monmouth Junction, NJ, USA; Catalog No. HY-13948) for 48 h, or 200 µM PA (MedChemExpress, Monmouth Junction, NJ, USA; Catalog No. HY-N0830) for 24 h to induce myofibroblast differentiation.

To evaluate the anti-fibrotic response of iCFBs, cells were treated for 48 h with medium containing 10 ng/mL TGF-β1 in combination with 10 µM N-[(1R)-1,2,3,4-tetrahydro-1-naphthalenyl]-1H-benzimidazol-2-amine (NS8593; MedChemExpress, Monmouth Junction, NJ, USA; Catalog No. HY-137952) or 1 mg/mL pirfenidone (PFD; MedChemExpress, Monmouth Junction, NJ, USA; Catalog No. HY-B0673).

2.11 Statistical Analysis

Data are presented as mean $\pm$ standard deviation (SD). Statistical analyses were performed using GraphPad Prism 8 software (GraphPad Software, San Diego, CA, USA).

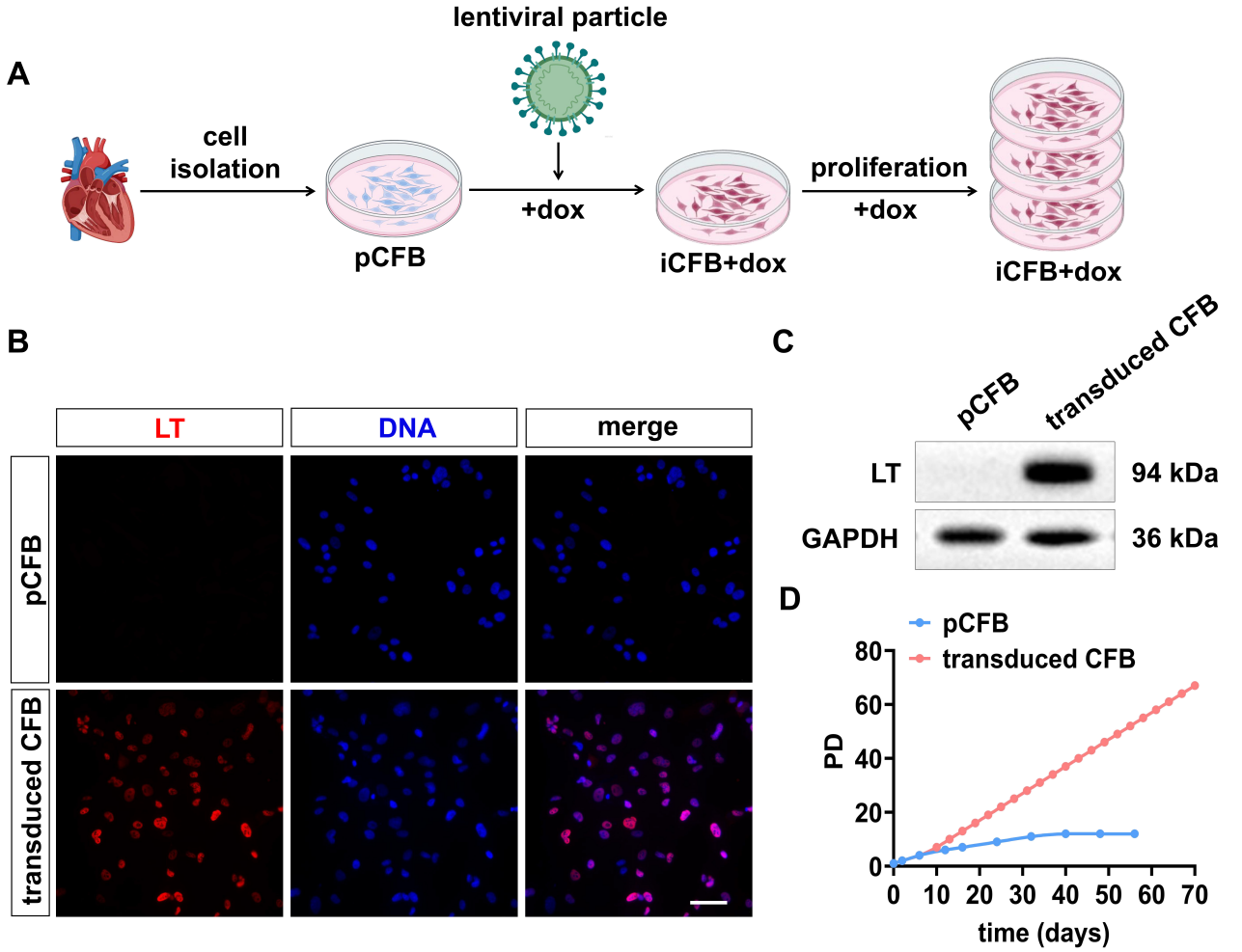

Fig. 1. Generation of conditionally immortalized cardiac fibroblasts (iCFBs). (A) Schematic overview of the conditional immortalization strategy. (B) Immunofluorescence staining confirming LT expression in transduced cardiac fibroblasts cultured in the presence of dox. Scale bar, 50 µm. (C) Western blot analysis confirming LT expression in transduced CFB cultured in the presence of dox. (D) Growth curves of pCFBs and transduced CFBs cultured in the presence of dox. CFB, cardiac fibroblast; pCFB, primary cardiac fibroblast; LT, SV40 large T antigen; GAPDH, glyceraldehyde-3-phosphate dehydrogenase; dox, doxycycline; PD, population doubling; iCFB+dox, iCFB cultured in the presence of dox; DNA, deoxyribonucleic acid. Created in BioRender. Liu, J. (2026) https://BioRender.com/iuxys2w.

One-way analysis of variance (ANOVA) followed by Bonferroni's post-hoc test was used for multiple group comparisons. All experiments were independently repeated at least thrice. Statistical significance was set at $p < 0.05$.

3. Results

3.1 iCFB Generation

To establish an iCFB line, pCFBs were transduced with lentiviral particles encoding a dox-inducible LT expression cassette under the control of the *COL1A2* promoter (Fig. 1A). Successful immortalization was confirmed by LT expression, which was robustly expressed in transduced cells (iCFBs) cultured in dox-containing medium, whereas no LT signal was detected in pCFBs (Fig. 1B,C).

Growth curve analysis demonstrated that pCFBs ceased to proliferate after approximately 9 population doublings (PDs). In contrast, iCFBs cultured in the presence of dox maintained sustained proliferation for over 70 PDs without entering senescence, with an average population doubling period of approximately 24 h (Fig. 1D). Taken together, these results confirmed the successful establishment of an iCFB line.

3.2 iCFBs Exhibit Dox-Dependent Proliferation

To determine whether LT expression and the associated immortalization phenotype in iCFBs were strictly dox-dependent, they were cultured in a medium switched from dox-containing to dox-free conditions (Fig. 2A). Western blot analysis confirmed LT expression in iCFBs maintained in dox-containing medium (day 0), with a time-dependent decline to undetectable levels by day 6 after dox withdrawal (Fig. 2B,C), which was further validated by immunofluo-

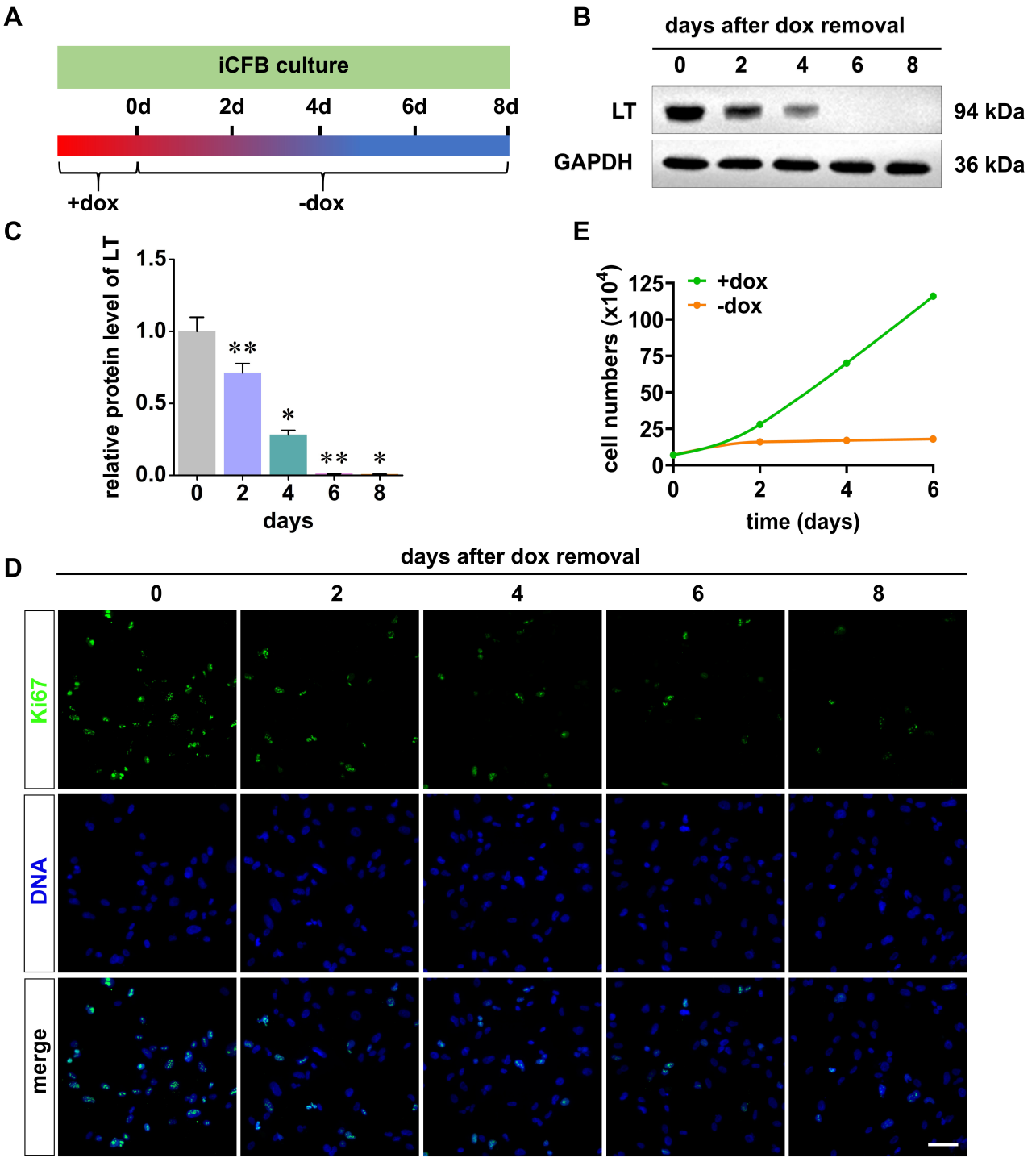

Fig. 2. Conditional proliferative capacity of conditionally immortalized cardiac fibroblasts (iCFBs). (A) Schematic illustration of iCFB preparation and dox withdrawal process. (B,C) Western blot analysis and corresponding quantification of LT protein expression in iCFBs before (day 0) and after (days 2, 4, 6, and 8) dox withdrawal. (D) Immunofluorescence staining of the proliferation marker Ki-67 in iCFBs before (day 0) and after (days 2, 4, 6, and 8) dox withdrawal. Scale bar, 50 µm. (E) Quantitative analysis of iCFB cell counts after culture in media with or without dox. iCFB, conditionally immortalized cardiac fibroblast; LT, SV40 large T antigen; GAPDH, glyceraldehyde-3-phosphate dehydrogenase; dox, doxycycline; Ki-67, Ki-67 antigen; DNA, deoxyribonucleic acid. Data were presented as mean ± standard deviation (SD; n = 3). Statistical analysis was performed using one-way analysis of variance (ANOVA) followed by Bonferroni's post-hoc test. *$p < 0.05$, **$p < 0.01$.

rescence staining (**Supplementary Fig. 1**). Consistent with the changes in LT expression, Ki-67 antigen (Ki-67) positivity was abundant in dox-cultured iCFBs, but decreased substantially after dox withdrawal (Fig. 2D). Accordingly, iCFBs proliferated continuously after dox treatment. In contrast, following dox removal, cell numbers plateaued after a modest initial increase within days 0–2 (Fig. 2E). Taken together, these findings demonstrate that dox tightly regulates both LT expression and proliferative capacity of iCFBs, enabling a reversible switch between an immortalized proliferative state and a non-immortalized phenotype.

3.3 iCFBs Maintain pCFB Identity

Next, we examined whether the iCFBs retained their phenotypic characteristics. We compared the expression of canonical CFB markers in iCFBs maintained under proliferative conditions with dox (iCFB+dox), iCFBs cultured without dox for 4 days to revert to a non-immortalized state (iCFB), and pCFBs. No significant differences were observed in the expression levels of key CFB marker genes, including the fibroblast-associated markers *COL1A1*, *DDR2*, *VIM*, and *POSTN*, as well as cardiac markers *GJA1* and *TBX20* between pCFBs and iCFBs (Fig. 3A). Notably, sustained exposure to dox (iCFB+dox) reduced the expression of these CFB-associated markers compared with that in both pCFBs and iCFBs (Fig. 3A).

Consistent with the transcriptional data, immunofluorescence staining verified comparable COL-1 and CX43 protein expression in pCFBs and dox-withdrawn iCFBs, confirming restoration of the pCFB molecular profile in iCFBs (Fig. 3B). FFBs, as non-cardiac fibroblast controls, expressed COL-1, but not CX43, further supporting the cardiac-specific identity of dox-withdrawn iCFBs (Fig. 3B). Taken together, these results indicate that, in the absence of dox-induced proliferative pressure, the molecular identity of iCFBs closely resemble that of pCFBs. Accordingly, iCFBs cultured for 4 d without dox were used for all subsequent functional experiments.

3.4 iCFBs Retain Key Functional Properties of pCFBs

A series of functional assays was performed to compare the biological behaviors of iCFBs and pCFBs. TGF-β1, a central mediator of cardiac fibrosis, is well known to induce myofibroblast transdifferentiation and to stimulate the production of collagen and α-smooth muscle actin (α-SMA). To evaluate myofibroblast differentiation, iCFBs were cultured in dox-free medium for 4 days to suppress LT expression; both iCFBs and pCFBs were then stimulated with TGF-β1 for 2 days.

Immunofluorescence analysis showed that TGF-β1 treatment markedly increased COL-1 expression in both cell types (Fig. 4A). Furthermore, α-SMA staining was localized to prominent stress fiber-like filaments that traversed the cytoplasm and aligned along the longitudinal axis of the cell. This characteristic fibrillar localization is a hallmark of mature contractile myofibroblasts, confirming the successful phenotypic conversion of iCFBs (Fig. 4A). Consistent with these observations, RT-qPCR analysis demonstrated that the mRNA levels of *COL1A1* and *ACTA2* (encoding α-SMA) were significantly elevated in differentiated iCFBs (iCFB-differentiated myofibroblasts, iCMFBs) and pCFBs (primary cardiac myofibroblasts, pCMFBs) compared to their undifferentiated controls (Fig. 4B).

Enhanced contractile activity is a hallmark of myofibroblast differentiation. In line with this, collagen gel contraction assays revealed that TGF-β1 stimulation induced significant gel contractions in iCFBs. The extent of contraction was comparable between iCFBs and pCFBs, with no statistically significant differences observed (Fig. 4C). Taken together, these functional analyses demonstrated that iCFBs retain a myofibroblast differentiation capacity that is highly similar to that of pCFBs.

3.5 iCFBs Maintain Phenotypic and Functional Fidelity During Long-Term Expansion

To assess the scalability of iCFBs as *in vitro* models, we examined their phenotypic stability and functional capacity during long-term subculture. Marker gene expression and TGF-β1-induced transdifferentiation were compared between iCFBs on PD30, iCFBs on PD60, and pCFBs. RT-qPCR analysis revealed highly consistent expression levels of the signature genes *COL1A1*, *POSTN*, *GJA1*, and *TBX20* across all three groups, indicating that iCFBs preserved their core molecular identity, even after continuous passaging to PD60 (Fig. 5A).

Immunofluorescence staining further demonstrated that iCFBs at both PD30 and PD60 displayed cellular morphology and expression patterns of COL-1 and CX43 that were highly similar to those observed in pCFBs, with no spontaneous differentiation (Fig. 5B).

After TGF-β1 treatment, all three groups (pCFB, iCFB-PD30, iCFB-PD60) successfully underwent myofibroblast differentiation with enhanced COL-1 deposition and α-SMA$^+$ stress fiber formation (Fig. 5C). RT-qPCR analysis further demonstrated that the expression levels of the fibrotic marker genes *COL1A1* and *ACTA2* in iCMFB-PD30 and iCMFB-PD60 cells were not significantly different from those in pCMFBs, suggesting that iCFBs maintained a robust and stable differentiation response despite long-term passaging (Fig. 5D).

Taken together, these results demonstrate that iCFBs maintain their core molecular identity and myofibroblast transdifferentiation potential after prolonged *in vitro* expansion.

3.6 iCFBs Serve as a Sensitive Platform for Pro-Fibrotic and Anti-Fibrotic Drug Screening

To evaluate the suitability of iCFB model for drug screening, we assessed its responsiveness to multiple pro-

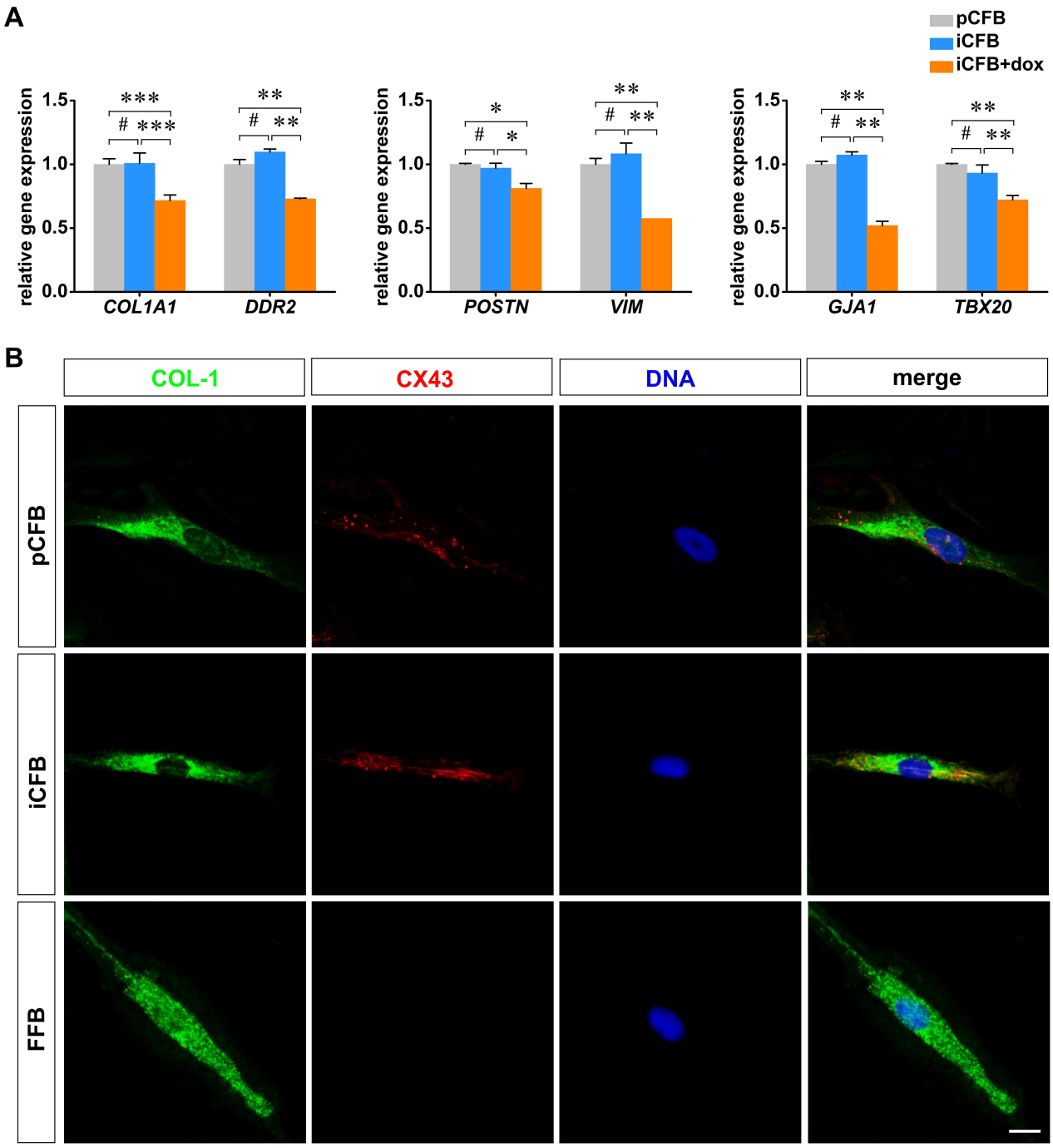

Fig. 3. Conditionally immortalized cardiac fibroblasts (iCFBs) retain primary cardiac fibroblast (pCFB) identity. (A) RT-qPCR analysis of fibroblast-associated marker genes (*COL1A1*, *DDR2*, *POSTN*, and *VIM*) and cardiac-specific genes (*GJA1* and *TBX20*) in pCFBs and iCFBs cultured in the presence or absence of dox. (B) Representative immunofluorescence images showing the expression of COL-1 (green) and CX43 (red) in iCFBs, pCFBs, and FFBs. Nuclei were counterstained with Hoechst 33342 (blue). Scale bar, 10 µm. RT-qPCR, reverse transcription-quantitative polymerase chain reaction; *COL1A1*, collagen type I alpha 1 chain; *DDR2*, discoidin domain receptor tyrosine kinase 2; *POSTN*, periostin; *VIM*, vimentin; *GJA1*, gap junction protein alpha 1; *TBX20*, T-box transcription factor 20; COL-1, Collagen type I; CX43, connexin 43; pCFB, primary cardiac fibroblast; iCFB, conditionally immortalized cardiac fibroblast; iCFB+dox, iCFB cultured in the presence of dox; FFB, foreskin fibroblast; DNA, deoxyribonucleic acid. Data were presented as mean ± standard deviation (SD; n = 3). Statistical analysis was performed using one-way ANOVA followed by Bonferroni's post-hoc test. *$p < 0.05$, **$p < 0.01$, ***$p < 0.001$; #not significant.

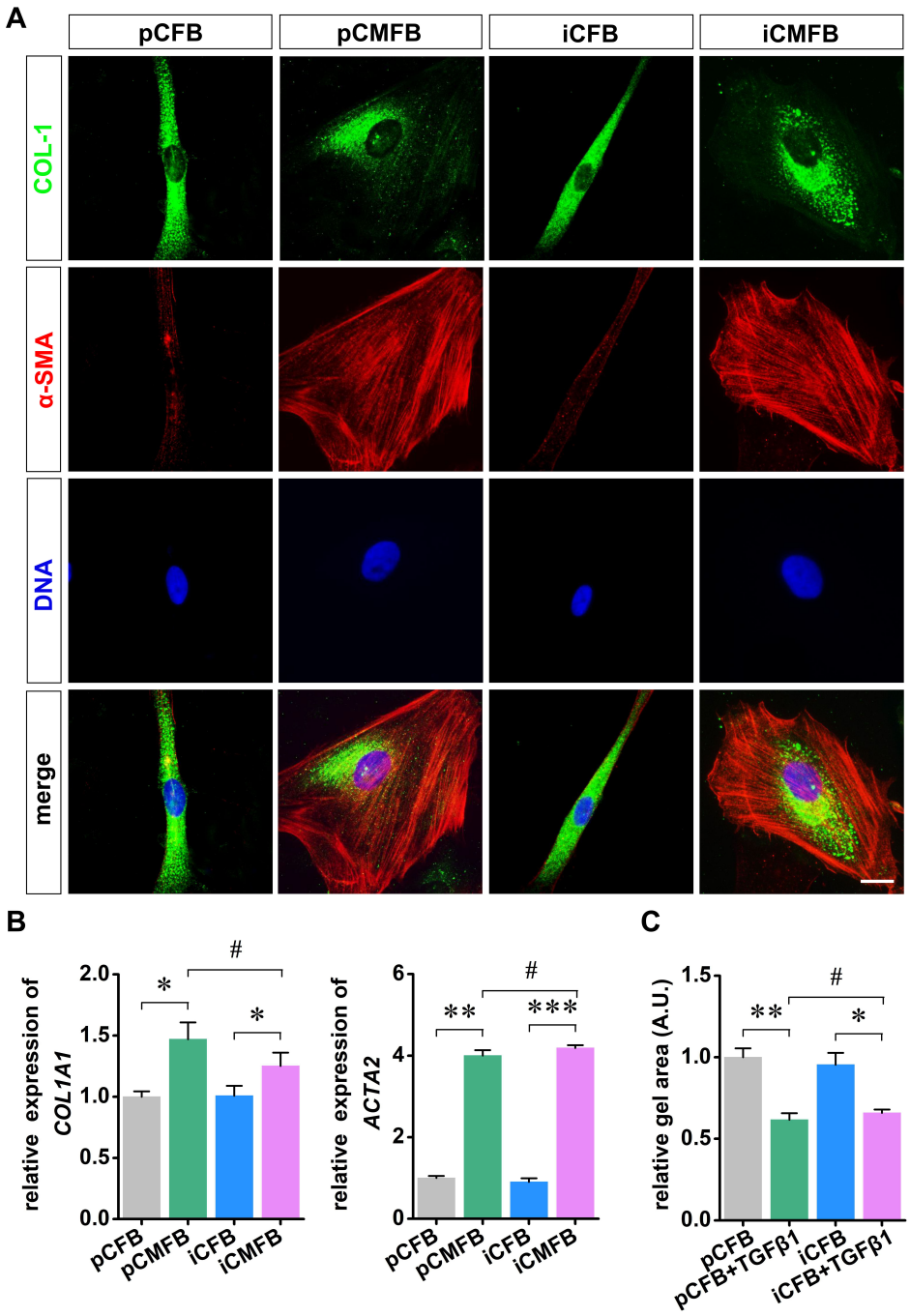

Fig. 4. Conditionally immortalized cardiac fibroblasts (iCFBs) retain key biological functions of primary cardiac fibroblasts (pCFBs). (A) Representative immunofluorescence images showing the expression of COL-1 (green) and α-SMA (red) in pCFBs, pCMFBs, iCFBs, and iCMFBs. Nuclei were counterstained with Hoechst 33342 (blue). Scale bar, 10 µm. (B) RT-qPCR analysis of *COL1A1* and *ACTA2* expression levels in pCFBs, pCMFBs, iCFBs, and iCMFBs. (C) Quantification of collagen gel contraction assays for each group. The remaining gel surface area was normalized to that of the pCFB control group. Gel area is inversely proportional to contractile activity. *COL1A1*, collagen type I alpha 1 chain; COL-1, collagen type I; *ACTA2*, actin alpha 2; α-SMA, α-smooth muscle actin; RT-qPCR, reverse transcription-quantitative polymerase chain reaction; pCFB, primary cardiac fibroblast; pCMFB, primary cardiac myofibroblast; iCFB, conditionally immortalized cardiac fibroblast; iCMFB, differentiated iCFBs; TGF-β1, transforming growth factor-β1; DNA, deoxyribonucleic acid. Data were presented as mean $\pm$ standard deviation (SD; n = 3). Statistical analysis was performed using one-way ANOVA followed by Bonferroni's post-hoc test. *$p < 0.05$, **$p < 0.01$, ***$p < 0.001$; #not significant.

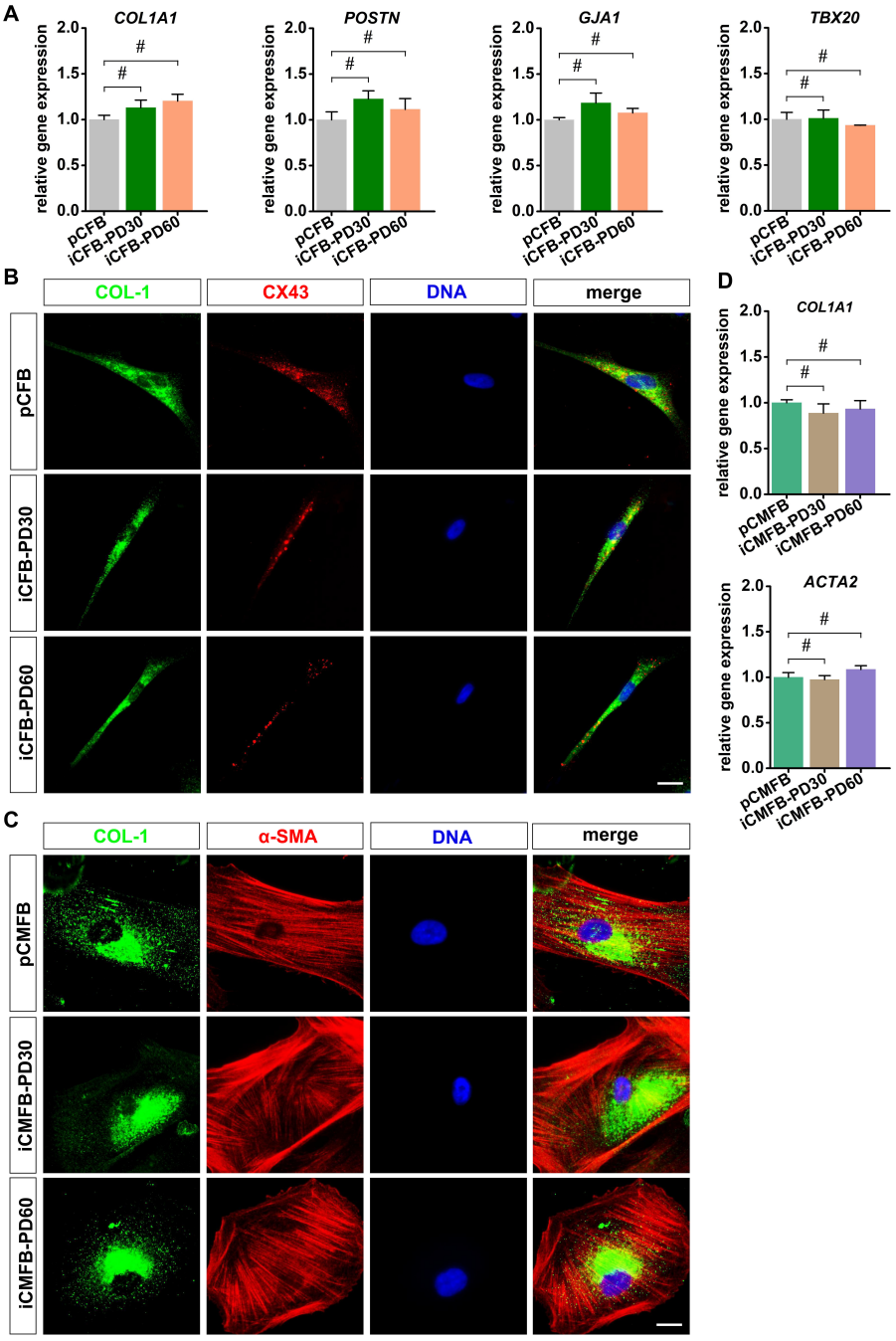

Fig. 5. Conditionally immortalized cardiac fibroblasts (iCFBs) preserve phenotypic and functional properties during long-term expansion. (A) RT-qPCR analysis of *COL1A1*, *POSTN*, *GJA1*, and *TBX20* expression levels in pCFBs and iCFBs at PD30 and PD60. (B) Representative immunofluorescence images showing COL-1 (green) and CX43 (red) expression in pCFBs and iCFBs at PD30 and PD60. Nuclei were counterstained with Hoechst 33342 (blue). Scale bar, 10 µm. (C) Representative immunofluorescence images showing COL-1 (green) and α-SMA (red) expression in pCMFB, iCMFB-PD30, and iCMFB-PD60. (D) RT-qPCR analysis of *COL1A1* and *ACTA2* expression levels in pCMFB, iCMFB-PD30, and iCMFB-PD60. Nuclei were counterstained with Hoechst 33342 (blue). Scale bar, 10 µm. COL-1, collagen type I; CX43, connexin 43; α-SMA, α-smooth muscle actin; *COL1A1*, collagen type I alpha 1 chain; *POSTN*, periostin; *GJA1*, gap junction protein alpha 1; *TBX20*, T-box transcription factor 20; *ACTA2*, actin alpha 2; RT-qPCR, reverse transcription-quantitative polymerase chain reaction; pCFB, primary cardiac fibroblast; iCFB, conditionally immortalized cardiac fibroblast; iCMFB, iCFB-differentiated myofibroblasts; pCMFB, primary cardiac myofibroblast; PD, population doubling; DNA, deoxyribonucleic acid. Data were presented as mean ± standard deviation (SD; n = 3). Statistical analysis was performed using one-way ANOVA followed by Bonferroni's post-hoc test. #not significant.

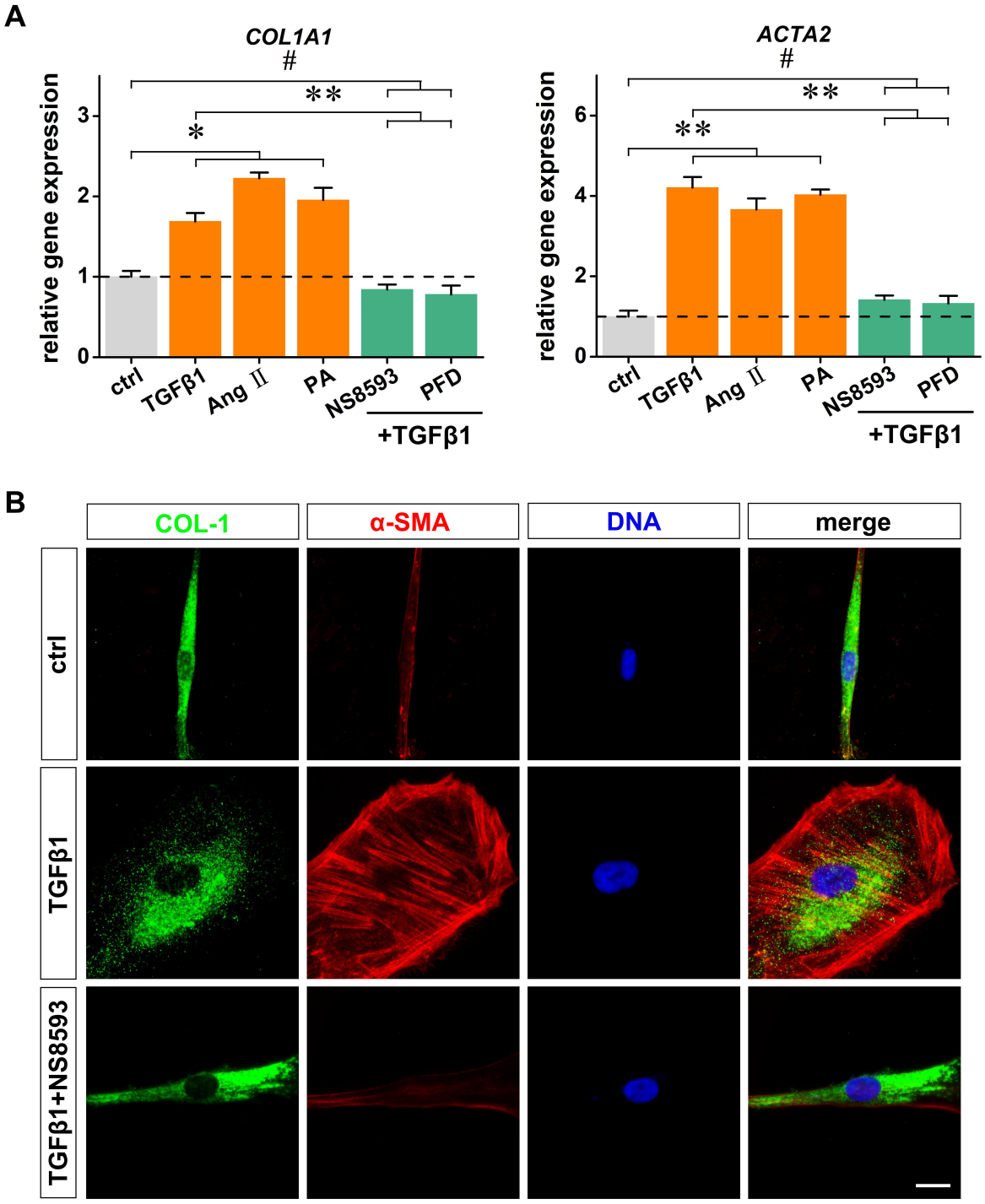

Fig. 6. Conditionally immortalized cardiac fibroblasts (iCFBs) serve as a platform for pro- and anti-fibrotic drug screening. (A) RT-qPCR analysis of myofibroblast marker gene expression (*COL1A1* and *ACTA2*) in iCFBs treated with pro-fibrotic stimuli (TGF-β1, Ang II, and PA) or TGF-β1 in combination with anti-fibrotic agents (NS8593 or PFD). Data were presented as mean ± standard deviation (SD; n = 3). (B) Representative immunofluorescence images showed COL-1 (green) and α-SMA (red) expression in iCFBs treated with TGF-β1 alone or in combination with NS8593. The nuclei were counterstained with Hoechst 33342 (blue). Scale bar, 10 µm. RT-qPCR, reverse transcription-quantitative polymerase chain reaction; *COL1A1*, collagen type I alpha 1 chain; *ACTA2*, actin alpha 2; COL-1, collagen type I; α-SMA, α-smooth muscle actin; ctrl, control; TGF-β1, transforming growth factor beta 1; Ang II, angiotensin II; PA, palmitic acid; NS8593, TRPM7 channel inhibitor; PFD, pirfenidone; DNA, deoxyribonucleic acid. Statistical analysis was performed using one-way ANOVA followed by Bonferroni's post-hoc test. *$p < 0.05$, **$p < 0.01$; #not significant.

fibrotic stimuli. After 4 days of culture in dox-free medium, iCFBs were treated with TGF-β1, Ang II, or PA to mimic the multifactorial pathways that contribute to cardiac fibrosis. Using *ACTA2* and *COL1A1* expression as readouts of fibroblast activation, we observed that all three stimuli significantly increased the levels of these fibrotic markers in iCFBs compared to that in the control conditions (Fig. 6A), indicating a robust induction of pro-fibrotic phenotypes *in vitro*.

Having established the broad pro-fibrotic responsiveness of the model, we examined its utility for evaluating anti-fibrotic compounds. Specifically, we tested whether the transient receptor potential melastatin 7 (TRPM7) channel antagonist NS8593 and the clinically approved anti-fibrotic drug PFD could suppress TGF-β1-induced myofibroblast transdifferentiation. Both NS8593 and PFD effectively attenuated the TGF-β1-induced *COL1A1* and *ACTA2* expression upregulation in iCFBs (Fig. 6A).

Consistent with these molecular findings, immunofluorescence analysis showed that TGF-β1-induced fibrotic morphological changes in iCFBs were significantly attenuated by NS8593 co-treatment (Fig. 6B). Collectively, these results indicated that the iCFB model is a reliable and sensitive *in vitro* platform for screening both pro-fibrotic stimuli and candidate anti-fibrotic therapeutics.

4. Discussion

In this study, we established and characterized an iCFB cell line as a scalable and phenotypically stable platform for studying fibrosis. A key feature of this model is its ability to respond to multiple pro-fibrotic stimuli, including TGF-β1, Ang II, and PA [23–25]. This multifactorial inducibility is relevant, as *in vivo* cardiac fibrosis results from the convergence of several pathogenic pathways [26,27]. Models activated by a single stimulus may not fully capture this complexity; therefore, the responsiveness of iCFBs to distinct inputs enhances their utility in drug screening.

Using this platform, we confirmed the anti-fibrotic effect of the TRPM7 inhibitor NS8593 [28], which attenuated TGF-β1-induced collagen deposition and marker gene expression in iCFBs. This finding is consistent with reports implicating TRPM7 in fibrotic signaling [29,30]. Although our data demonstrate the functional consequences of TRPM7 inhibition, the precise mechanism potentially involving Smad2/3 phosphorylation, as suggested by previous studies, requires further investigation [31].

We also observed that PFD significantly suppressed TGF-β1-induced fibrotic responses in iCFBs, consistent with its known mechanisms of inhibiting fibroblast activation [32,33]. These findings support the idea that fibrotic diseases in different organs share core pathological pathways [34]. Owing to their established safety profile in humans [35], this study provides pre-clinical evidence supporting the repurposing of PFD for treating cardiac fibrosis.

Conditional immortalization offers a practical advantage over permanent methods. Proliferation is tightly controlled by dox. Upon withdrawal, iCFBs exit the cell cycle and re-express key cardiac fibroblast markers (*COL1A1*, *POSTN*, *GJA1*, *TBX20*) at levels comparable to those in primary cells. This reversible system allows scalable expansion while enabling experiments to be performed on cells in a quiescent, primary-like state, thereby avoiding the phenotypic drift often observed in constitutively immortalized lines.

This model also demonstrates long-term stability. The iCFBs retained their molecular identity and differentiation capacity even at high passage numbers (up to PD60). This consistency addresses the limitation of primary cultures, namely senescence and batch-to-batch variability, and supports the use of iCFBs in reproducible large-scale screening applications.

5. Limitations

This study has several limitations. First, as a monocellular *in vitro* model, iCFBs cannot fully recapitulate the complex *in vivo* microenvironment of the fibrotic myocardium, which involves dynamic interactions between multiple cell types (such as cardiomyocytes, immune cells, and endothelial cells), biomechanical cues, and paracrine signaling networks.

Second, iCFBs are derived from fetal cardiac ventricular tissue and therefore may not fully reflect the phenotypic and functional characteristics of adult CFBs, which primarily mediate fibrotic remodeling in adult heart failure and myocardial injury. Fetal and adult cardiac fibroblasts exhibit distinct molecular profiles, proliferative capacities, and responsiveness to pro-fibrotic stimuli. This difference may limit the direct translational relevance of the findings obtained using this fetus-derived model in adult cardiac fibrosis.

Third, our drug screening assessments were based on short-term *in vitro* exposure and did not evaluate long-term functional outcomes or potential off-target effects. Therefore, the findings of this model require further validation in more physiologically relevant systems, including *ex vivo* models, *in vivo* animal studies, and clinical investigations. Future studies using adult-derived iCFBs and co-culture systems incorporating multiple cardiac cell types will enhance the translational relevance of this platform.

6. Conclusion

In conclusion, we successfully established a conditionally immortalized human CFB line as a novel and superior *in vitro* model for cardiac fibrosis research. The core innovation lies in dox-controlled reversible immortalization, which provides unlimited scalability and allows cells to revert to a primary-like quiescent state for functional assays, a critical advantage over permanently immortalized lines that often suffer from phenotypic drift. Comprehensive charac-

terization confirmed that iCFBs maintained the key molecular identity, long-term stability, and differentiation potential of primary fibroblasts. Furthermore, we validated the broad applicability of the model by demonstrating its robust activation by multiple pathogenic stimuli and its utility for evaluating both novel target (NS8593) and repurposed (PFD) anti-fibrotic compounds. This work not only provides a reliable and standardized cellular platform to overcome the limitations of primary cell sourcing, but also opens efficient pathways for both *de novo* drug discovery and drug repurposing for treating cardiac fibrosis. Therefore, the iCFB model holds substantial promise for enhancing the precision and throughput of pre-clinical development of much-needed anti-fibrotic therapies.

Availability of Data and Materials

All data and materials are available from the corresponding author upon reasonable request.

Author Contributions

SW and RH designed the experiments. SW, RG, and CW performed the experiments. SW, CW, and WK analyzed the data. RH, JL, and CL contributed to data interpretation and manuscript revision. RH, JL, and CL wrote the paper. All authors contributed to editorial changes in the manuscript. All authors read and approved the final manuscript. All authors have participated sufficiently in the work and agreed to be accountable for all aspects of the work.

Ethics Approval and Consent to Participate

This study was approved by the Ethics Committee of Longgang District People's Hospital of Shenzhen, with the approval number: 2025101. The study was carried out in accordance with the guidelines of the Declaration of Helsinki. And obtained the corresponding written informed consent from the fetal parents.

Acknowledgment

We thank Mrs. Lei Zhang from Longgang District People's Hospital of Shenzhen for her administrative assistance.

Funding

This work was granted by the Shenzhen Science and Technology Innovation Program (No. JCYJ20230807141801002 and JCYJ20240813160259020) and the Longgang District Science and Technology Innovation Bureau Project (LGKCYLWS2022025). This work was supported by the Longgang District Key Specialty Program.

Conflicts of Interest

The authors declare no conflicts of interest.

Supplementary Material

Supplementary material associated with this article can be found, in the online version, at https://doi.org/10.31083/FBL49465.

References

[1] Tallquist MD. Cardiac Fibroblast Diversity. Annual Review of Physiology. 2020; 82: 63–78. https://doi.org/10.1146/annurev-physiol-021119-034527.

[2] Souders CA, Bowers SLK, Baudino TA. Cardiac fibroblast: the renaissance cell. Circulation Research. 2009; 105: 1164–1176. https://doi.org/10.1161/CIRCRESAHA.109.209809.

[3] Dostal D, Glaser S, Baudino TA. Cardiac fibroblast physiology and pathology. Comprehensive Physiology. 2015; 5: 887–909. https://doi.org/10.1002/cphy.c140053.

[4] Gourdie RG, Dimmeler S, Kohl P. Novel therapeutic strategies targeting fibroblasts and fibrosis in heart disease. Nature Reviews. Drug Discovery. 2016; 15: 620–638. https://doi.org/10.1038/nrd.2016.89.

[5] Weber KT, Sun Y, Bhattacharya SK, Ahokas RA, Gerling IC. Myofibroblast-mediated mechanisms of pathological remodelling of the heart. Nature Reviews. Cardiology. 2013; 10: 15–26. https://doi.org/10.1038/nrcardio.2012.158.

[6] Porter KE, Turner NA. Cardiac fibroblasts: at the heart of myocardial remodeling. Pharmacology & Therapeutics. 2009; 123: 255–278. https://doi.org/10.1016/j.pharmthera.2009.05.002.

[7] Frangogiannis NG. Cardiac fibrosis: Cell biological mechanisms, molecular pathways and therapeutic opportunities. Molecular Aspects of Medicine. 2019; 65: 70–99. https://doi.org/10.1016/j.mam.2018.07.001.

[8] Lunde IG, Rypdal KB, Van Linthout S, Diez J, González A. Myocardial fibrosis from the perspective of the extracellular matrix: Mechanisms to clinical impact. Matrix Biology. 2024; 134: 1–22. https://doi.org/10.1016/j.matbio.2024.08.008.

[9] Leask A. Getting to the heart of the matter: new insights into cardiac fibrosis. Circulation Research. 2015; 116: 1269–1276. https://doi.org/10.1161/CIRCRESAHA.116.305381.

[10] Burke RM, Burgos Villar KN, Small EM. Fibroblast contributions to ischemic cardiac remodeling. Cellular Signalling. 2021; 77: 109824. https://doi.org/10.1016/j.cellsig.2020.109824.

[11] Ishiura J, Nakamori S, Ishida M, Dohi K. 'Targeting the cardiac myocyte and fibrosis' in heart failure. European Heart Journal. 2022; 43: 432. https://doi.org/10.1093/eurheartj/ehab780.

[12] López B, Ravassa S, Moreno MU, José GS, Beaumont J, González A, *et al*. Diffuse myocardial fibrosis: mechanisms, diagnosis and therapeutic approaches. Nature Reviews. Cardiology. 2021; 18: 479–498. https://doi.org/10.1038/s41569-020-00504-1.

[13] Chimenti I, Pagano F, Cozzolino C, Icolaro F, Floris E, Picchio V. The Role of Cardiac Fibroblast Heterogeneity in Myocardial Fibrosis and Its Novel Therapeutic Potential. International Journal of Molecular Sciences. 2025; 26: 5882. https://doi.org/10.3390/ijms26125882.

[14] Cinato M, Kang R, Kramar S, Savchenko L, Pizzinat N, Swiader A, *et al*. Transcriptome fingerprinting of aberrant fibroblast activation unlocks effective therapeutics to tackle cardiac fibrosis. Science Advances. 2025; 11: eadx0968. https://doi.org/10.1126/sciadv.adx0968.

[15] Meng XY, Li Y , Meng LB, Yang CG, Xia CX, Wang X, *et al*. Growth Differentiation Factor 15 Inhibits Cardiac Fibrosis, Oxidative Stress, Inflammation, and Apoptosis in a Rat Model of Heart Failure with Preserved Ejection Fraction. Front. Biosci. (Landmark Ed). 2025; 30: eadx26857. https://doi.org/10.31083/FBL26857.

[16] Fang L, Murphy AJ, Dart AM. A Clinical Perspective of Anti-Fibrotic Therapies for Cardiovascular Disease. Frontiers in Pharmacology. 2017; 8: 186. https://doi.org/10.3389/fphar.2017.00186.

[17] Spoladore R, Falasconi G, Fiore G, Di Maio S, Preda A, Slavich M, *et al*. Cardiac fibrosis: emerging agents in preclinical and clinical development. Expert Opinion on Investigational Drugs. 2021; 30: 153–166. https://doi.org/10.1080/13543784.2021.1868432.

[18] Zhao M, Wang L, Wang M, Zhou S, Lu Y, Cui H, *et al*. Targeting fibrosis, mechanisms and cilinical trials. Signal Transduction and Targeted Therapy. 2022; 7: 206. https://doi.org/10.1038/s41392-022-01070-3.

[19] Kel A, Thum T, Kunduzova O. Targeting fibroblast phenotype switching in cardiac remodelling as a promising antifibrotic strategy. European Heart Journal. 2025; 46: 354–358. https://doi.org/10.1093/eurheartj/ehae722.

[20] Xu Q, Norman JT, Shrivastav S, Lucio-Cazana J, Kopp JB. In vitro models of TGF-beta-induced fibrosis suitable for high-throughput screening of antifibrotic agents. American Journal of Physiology. Renal Physiology. 2007; 293: F631–F640. https://doi.org/10.1152/ajprenal.00379.2006.

[21] Liao G, Long C, Guo R, Wang S, Han R, Yang J, *et al*. Conditional immortalization of mesenchymal stem cells and their extracellular vesicles therapy for interstitial cystitis/bladder pain syndrome. Stem Cell Research & Therapy. 2025; 16: 459. https://doi.org/10.1186/s13287-025-04615-9.

[22] Liu J, Volkers L, Jangsangthong W, Bart CI, Engels MC, Zhou G, *et al*. Generation and primary characterization of iAM-1, a versatile new line of conditionally immortalized atrial myocytes with preserved cardiomyogenic differentiation capacity. Cardiovascular Research. 2018; 114: 1848–1859. https://doi.org/10.1093/cvr/cvy134.

[23] Jiménez-González S, Marín-Royo G, Jurado-López R, Bartolomé MV, Romero-Miranda A, Luaces M, *et al*. The Crosstalk between Cardiac Lipotoxicity and Mitochondrial Oxidative Stress in the Cardiac Alterations in Diet-Induced Obesity in Rats. Cells. 2020; 9: 451. https://doi.org/10.3390/cells9020451.

[24] Bujak M, Frangogiannis NG. The role of TGF-beta signaling in myocardial infarction and cardiac remodeling. Cardiovascular Research. 2007; 74: 184–195. https://doi.org/10.1016/j.cardiores.2006.10.002.

[25] Jana S, Aujla P, Hu M, Kilic T, Zhabyeyev P, McCulloch CA, *et al*. Gelsolin is an important mediator of Angiotensin II-induced activation of cardiac fibroblasts and fibrosis. FASEB Journal. 2021; 35: e21932. https://doi.org/10.1096/fj.202100038RR.

[26] Maruyama K, Imanaka-Yoshida K. The Pathogenesis of Cardiac Fibrosis: A Review of Recent Progress. International Journal of Molecular Sciences. 2022; 23: 2617. https://doi.org/10.3390/ijms23052617.

[27] Bacmeister L, Schwarzl M, Warnke S, Stoffers B, Blankenberg S, Westermann D, *et al*. Inflammation and fibrosis in murine models of heart failure. Basic Research in Cardiology. 2019; 114: 19. https://doi.org/10.1007/s00395-019-0722-5.

[28] Chubanov V, Gudermann T. Mapping TRPM7 Function by NS8593. International Journal of Molecular Sciences. 2020; 21: 7017. https://doi.org/10.3390/ijms21197017.

[29] Rios FJ, Zou ZG, Harvey AP, Harvey KY, Nosalski R, Anyfanti P, *et al*. Chanzyme TRPM7 protects against cardiovascular inflammation and fibrosis. Cardiovascular Research. 2020; 116: 721–735. https://doi.org/10.1093/cvr/cvz164.

[30] Suzuki S, Penner R, Fleig A. TRPM7 contributes to progressive nephropathy. Scientific Reports. 2020; 10: 2333. https://doi.org/10.1038/s41598-020-59355-y.

[31] Hu F, Li M, Han F, Zhang Q, Zeng Y, Zhang W, *et al*. Role of TRPM7 in cardiac fibrosis: A potential therapeutic target (Review). Experimental and Therapeutic Medicine. 2021; 21: 173. https://doi.org/10.3892/etm.2020.9604.

[32] Li N, Hang W, Shu H, Zhou N. Pirfenidone alleviates cardiac fibrosis induced by pressure overload via inhibiting TGF-β1/Smad3 signalling pathway. Journal of Cellular and Molecular Medicine. 2022; 26: 4548–4555. https://doi.org/10.1111/jcmm.17478.

[33] Aimo A, Spitaleri G, Panichella G, Lupón J, Emdin M, Bayes-Genis A. Pirfenidone as a novel cardiac protective treatment. Heart Failure Reviews. 2022; 27: 525–532. https://doi.org/10.1007/s10741-021-10175-w.

[34] Henderson NC, Rieder F, Wynn TA. Fibrosis: from mechanisms to medicines. Nature. 2020; 587: 555–566. https://doi.org/10.1038/s41586-020-2938-9.

[35] King TE Jr, Bradford WZ, Castro-Bernardini S, Fagan EA, Glaspole I, Glassberg MK, *et al*. A phase 3 trial of pirfenidone in patients with idiopathic pulmonary fibrosis. The New England Journal of Medicine. 2014; 370: 2083–2092. https://doi.org/10.1056/NEJMoa1402582.